

Supporting information

for

Hydrogen spillover for boosted catalytic activity towards hydrazine oxidation

Shuyuan Pan^a, Yuhua Xie^a, Chen Li^{b*}, Chunsheng Li^{c,d}, Yan Sun^{c,d*} and Zehui Yang^{a*}

^aFaculty of Materials Science and Chemistry, China University of Geosciences Wuhan, 388 Lumo RD, Wuhan, 430074, China.

^bCollege of Materials Science and Engineering, State Key Laboratory of New Textile Materials & Advanced Processing Technology, Wuhan Textile University, Wuhan, 430200, China.

^cSchool of Chemistry and Life Sciences, Suzhou University of Science and Technology, Suzhou City, Jiangsu Province 215009, China.

^dKey Laboratory of Advanced Electrode Materials for Novel Solar Cells for Petroleum and Chemical Industry of China, Suzhou University of Science and Technology, Suzhou City, Jiangsu Province 215009, China.

Experimental section

Materials and chemicals: Rhodium acetylacetonate ($\text{Rh}(\text{acac})_3$, 97%), Bis(acetylacetonato)- dioxomolybdenum ($\text{MoO}_2(\text{acac})_2$, 97%), formaldehyde (37 wt. % in H_2O), Carbon black (Vulcan XC-72), Nafion solution (5 wt%).

Synthesis of $\text{MoO}_2\text{-Rh-NF}$: 20 mg $\text{Rh}(\text{acac})_3$ and 10 mg $\text{MoO}_2(\text{acac})_2$ were dispersed in 8 mL ultrapure water, and 5 mL formaldehyde was added after stirring for 30 min at room temperature. The solution was then transferred to a stainless-steel autoclave lined with Teflon. It was heated from room temperature to 180 °C and held for 10 h. After cooling the autoclave to room temperature, the product was washed more than three times with ethanol to remove organic matter and then dried in a vacuum oven at 65 °C for 10 h. MoO_2 , Rh-NF were obtained without the addition of rhodium or molybdenum sources, respectively.

Fundamental characterization: Bruker (D8 Focus) was used for XRD test. The XPS images were collected by Escalab 250Xi (Thermo Scientific). The TEM images were acquired by JEOL JEM 2100F. The SEM image was taken by HITACHI SU8010.

Electrochemical measurement: In electrochemical testing, glassy carbon electrode (GCE), graphitic rod and Hg/HgO were utilized as work, counter and reference electrodes, respectively. The electrolyte was the 1.0 M KOH filled with N_2 . The polarization curves were measured at the sweep of 5 mV/s. The electrochemical impedance spectroscopy was recorded at a potential of 10 mA cm^{-2} . Cyclic voltammetry was used to cycle between -0.05 and 0.15 V vs. RHE at the sweep of 100 mV/s, and the polarization curves before and after the cycle were compared to

characterize the durability.

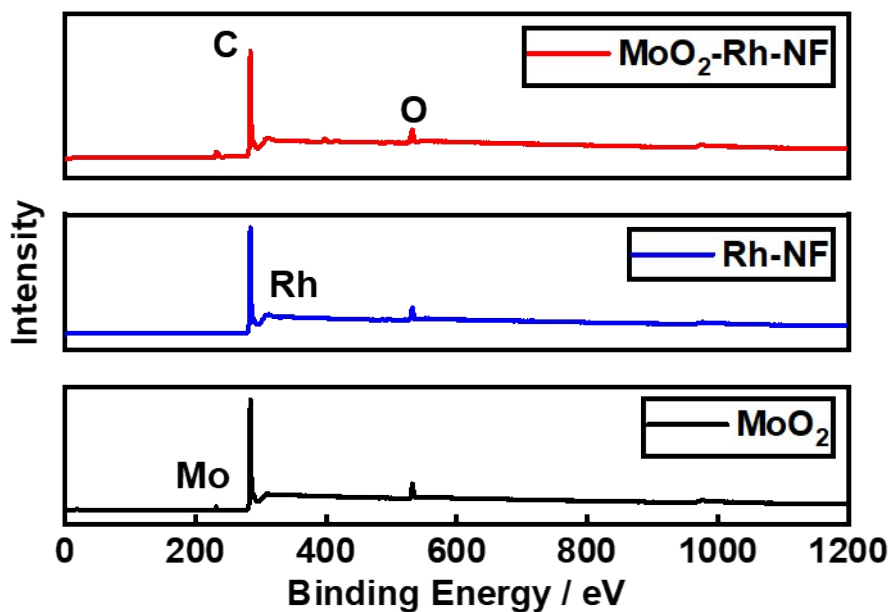


Figure S1 XPS survey scan of MoO₂-Rh-NF and Rh-NF electrocatalysts.

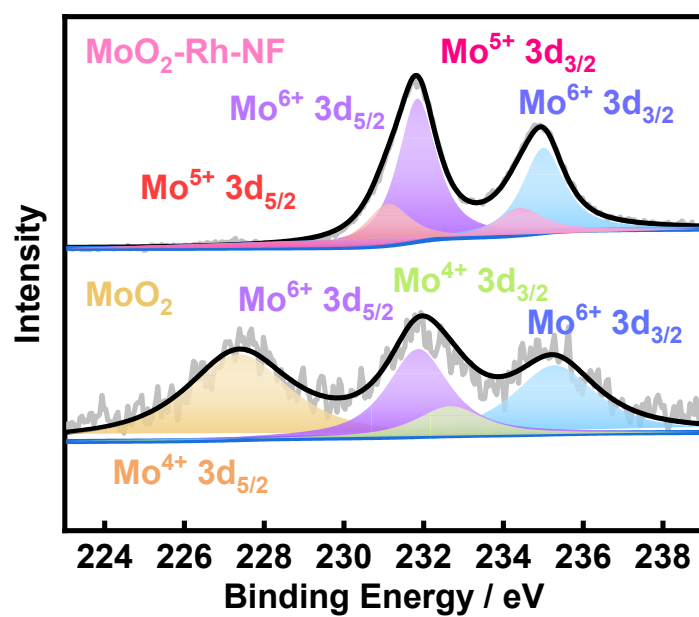


Figure S2 Mo 3d XPS spectrum of MoO₂-Rh-NF and Rh-NF electrocatalysts.

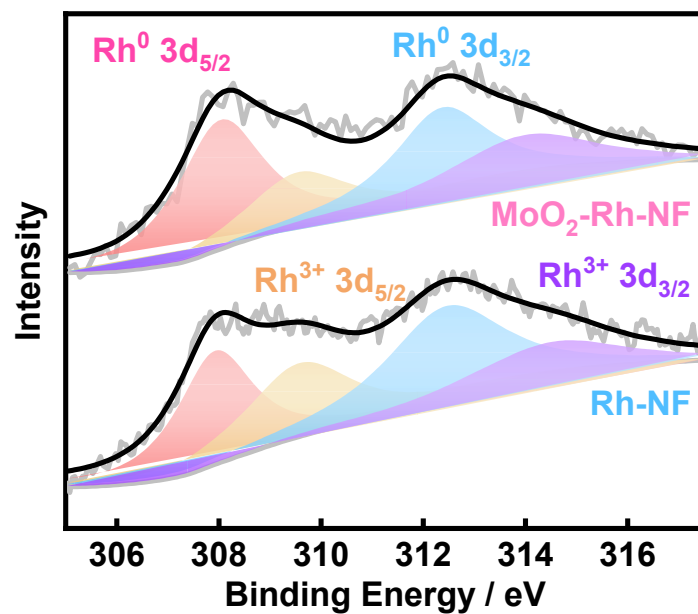


Figure S3 Rh 3d XPS spectrum of MoO₂-Rh-NF and Rh-NF electrocatalysts.

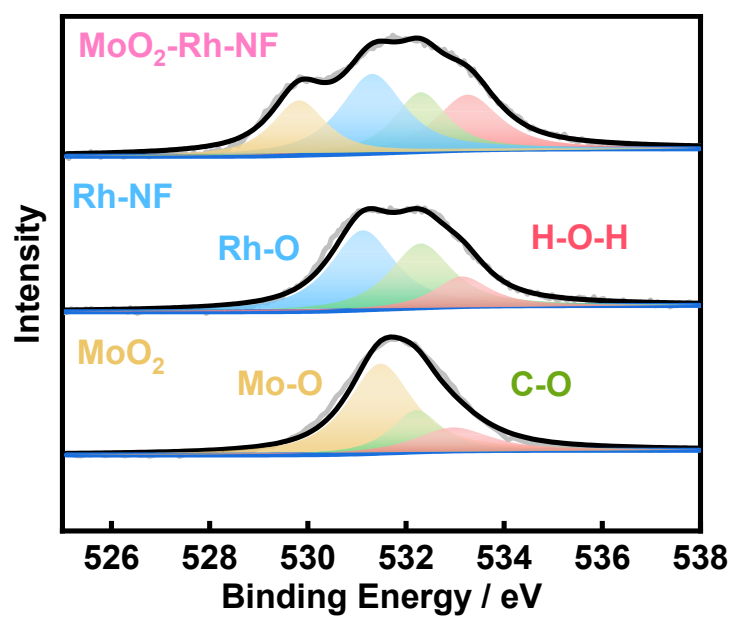


Figure S4 O 1s XPS spectrum of MoO₂-Rh-NF and Rh-NF electrocatalysts.

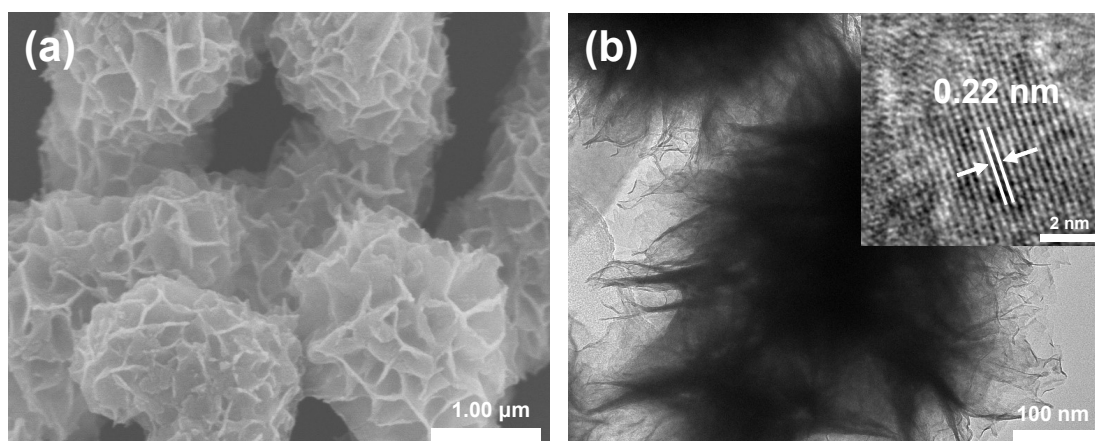


Figure S5 (a) SEM image, (b) TEM image and HAADF-STEM image of Rh-NF.

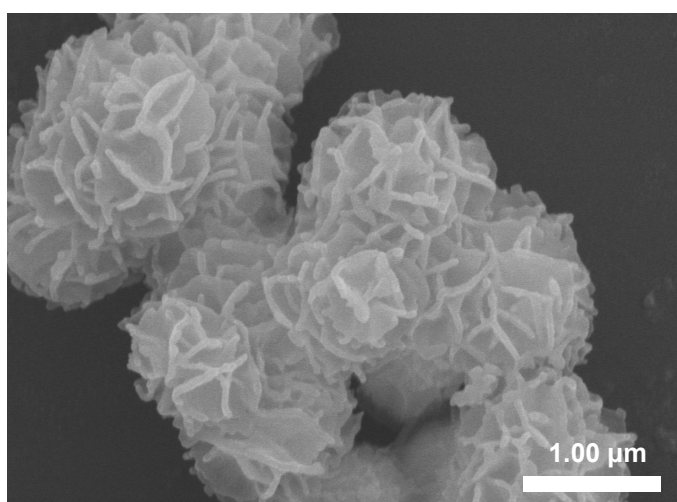


Figure S6 SEM image of MoO₂-Rh-NF.

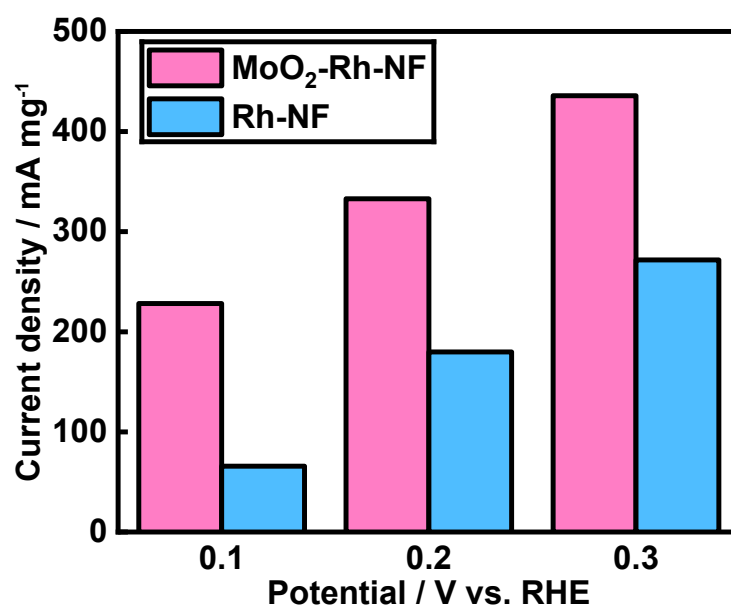


Figure S7 (a) Mass activities of MoO₂-Rh-NF and Rh-NF.

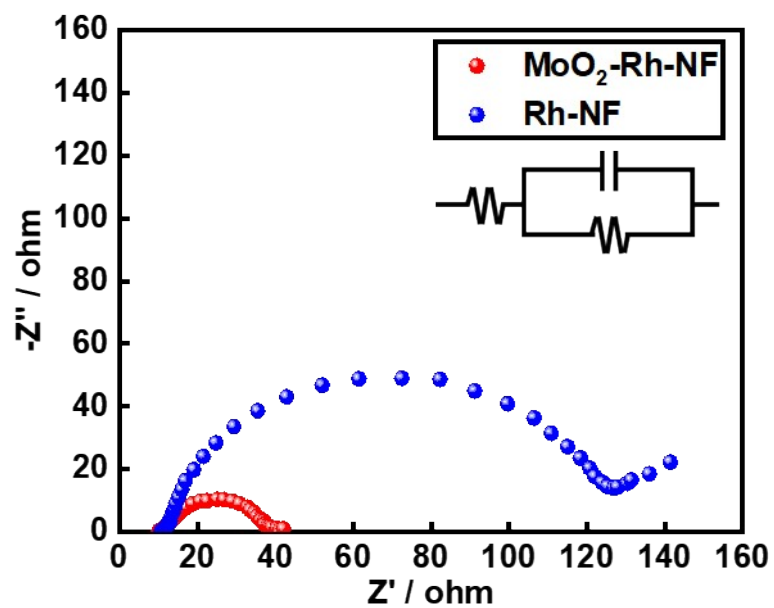


Figure S8 (a) EIS of MoO₂-Rh-NF and Rh-NF.

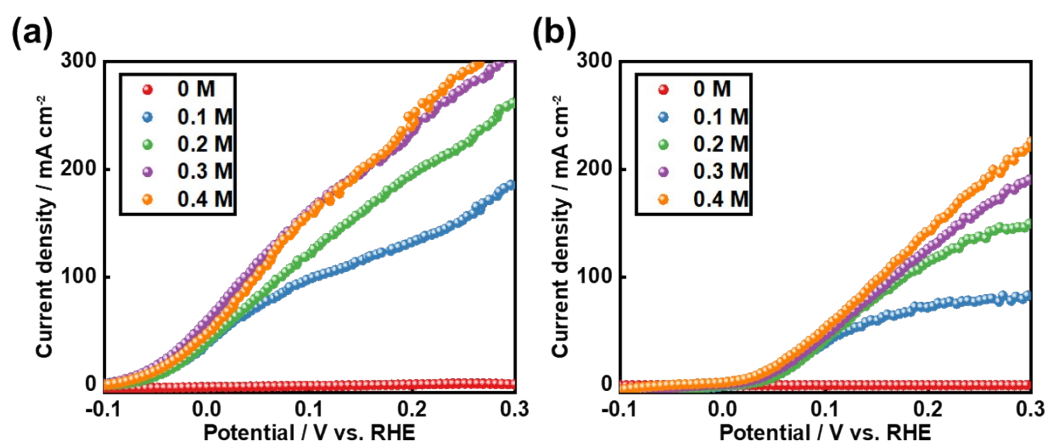


Figure S9 Polarization curves of MoO₂-Rh-NF (a) and Rh-NF (b) in different contents of hydrazine.

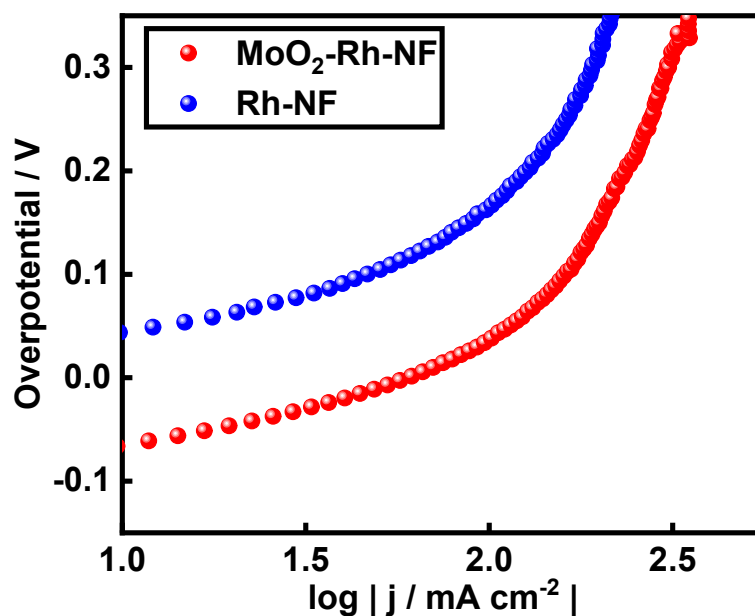


Figure S10 (a) Tafel slopes of MoO₂-Rh-NF and Rh-NF in the range of 100-200 mA cm⁻².

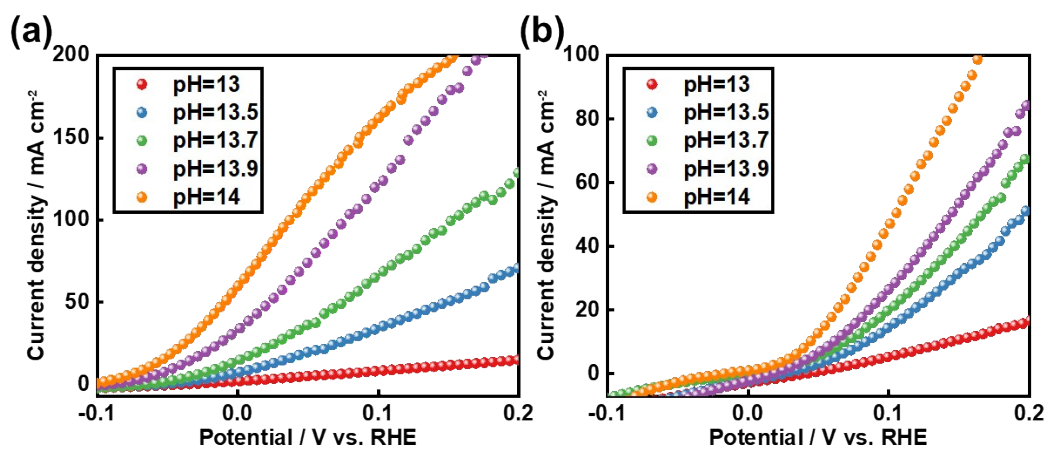


Figure S11 Polarization curves of MoO₂-Rh-NF (a) and Rh-NF (b) in different pH.

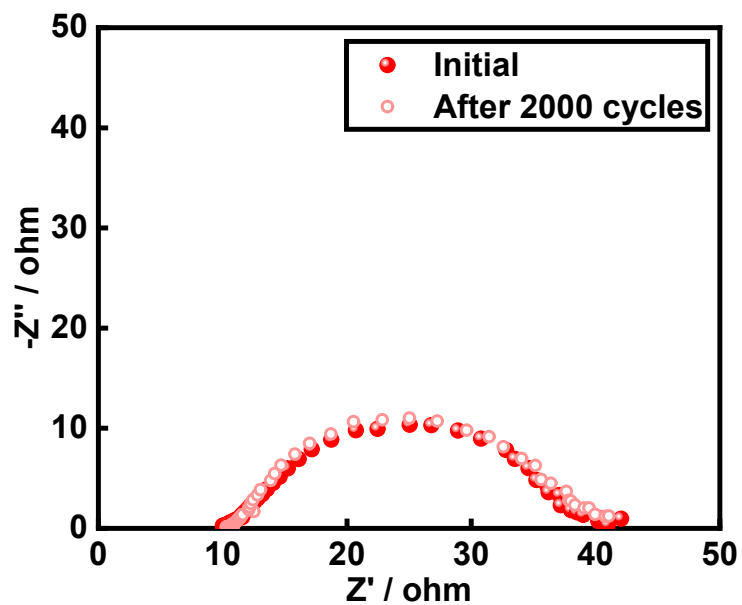


Figure S12 (a) EIS of MoO₂-Rh-NF before and after 2000 cycles.

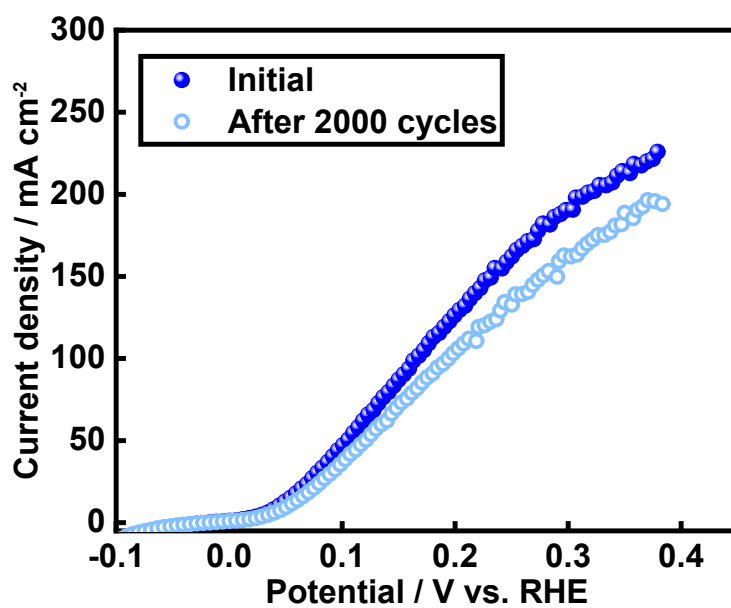


Figure S13 (a) Polarization curves for Rh-NF after 2000 cycles.

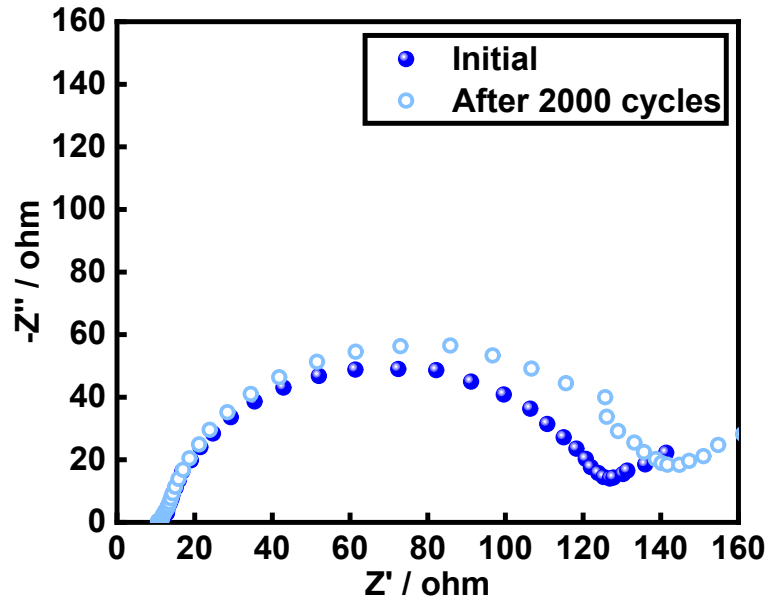


Figure S14 (a) EIS of Rh-NF before and after 2000 cycles.

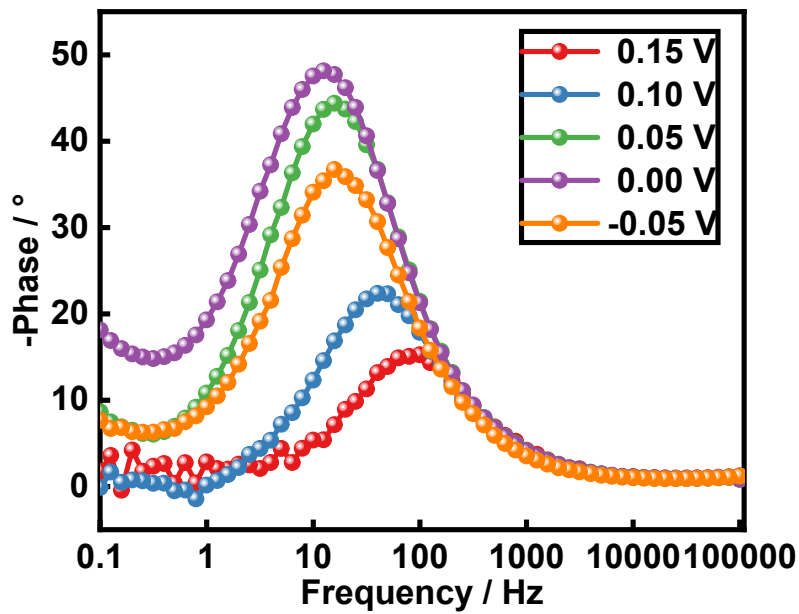


Figure S15 (a) Phase angles of Rh-NF at different potentials.

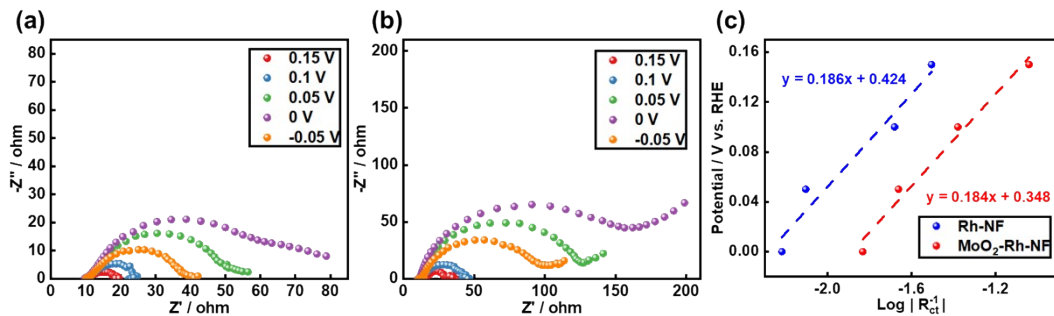


Figure S16 EIS of MoO₂-Rh-NF (a) and Rh-NF (b) at various potentials. (c) EIS-

derived Tafel plots of the MoO₂-Rh-NF and Rh-NF catalysts obtained from the R_{ct}.

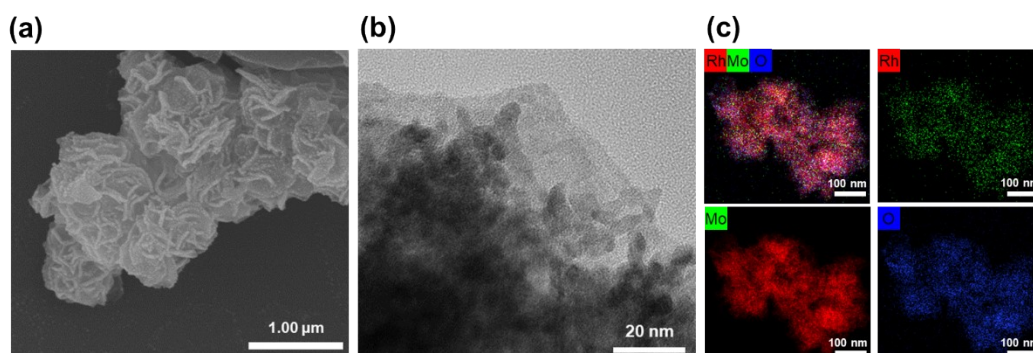


Figure S17 SEM, TEM and HAADF-STEM image for MoO₂-Rh-NF after stability

test.

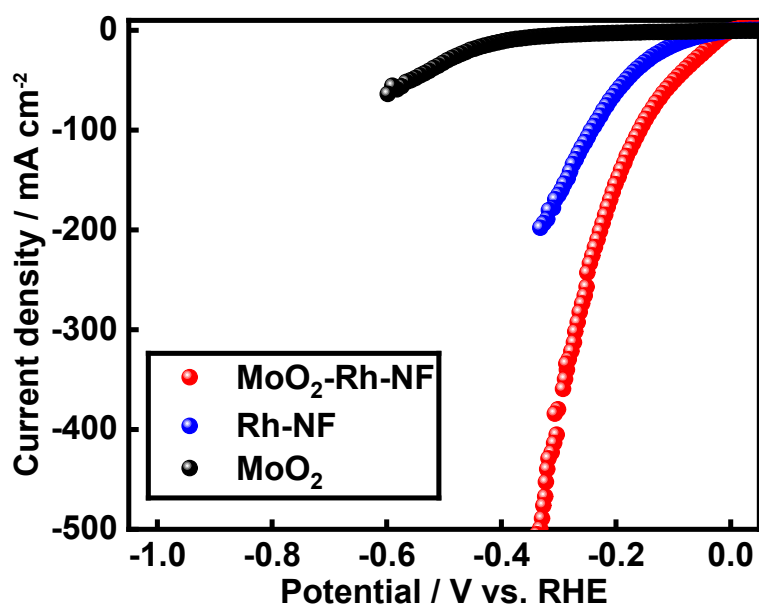


Figure S18 HER performance of MoO₂-Rh in 1 M KOH.

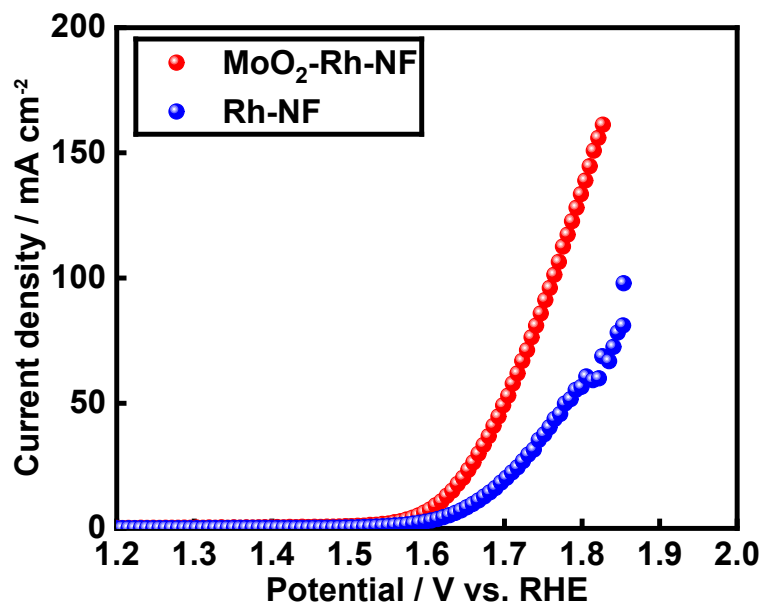


Figure S19 OER performance of MoO₂-Rh-NF and Rh-NF in 1 M KOH.

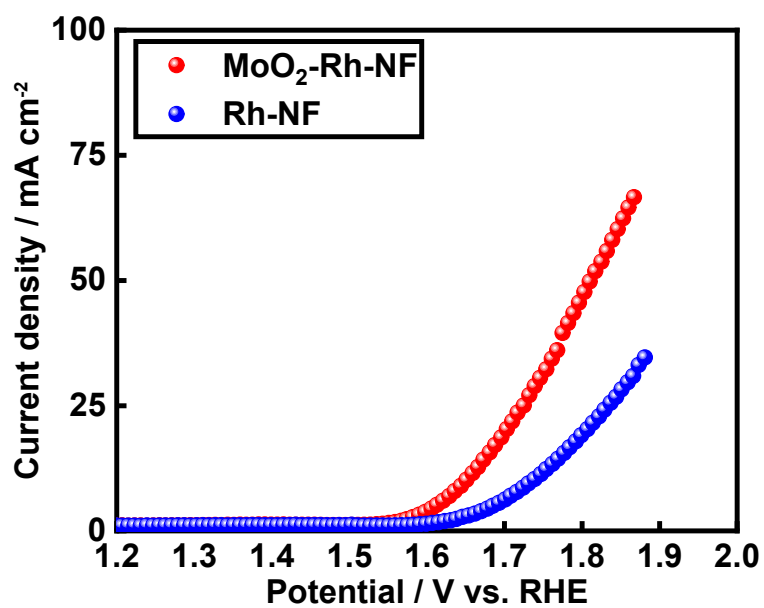


Figure S20 Performance of MoO₂-Rh-NF and Rh-NF in 1 M KOH for HER-OER system.

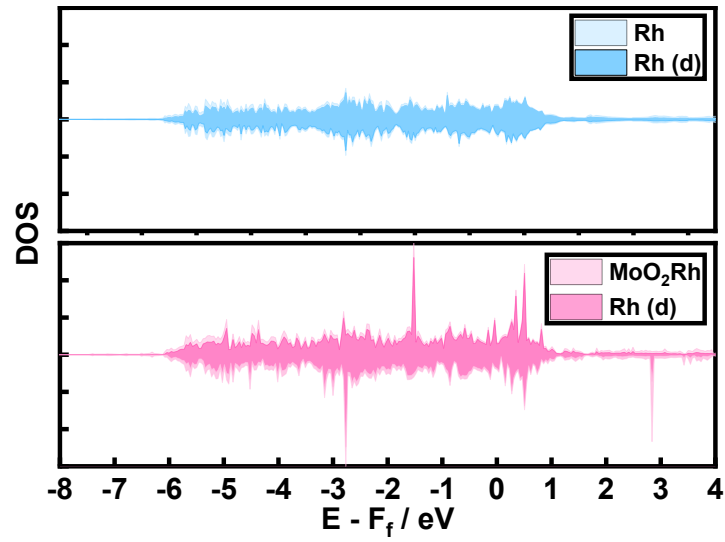


Figure S21 Density of state of Rh and MoO₂-Rh.

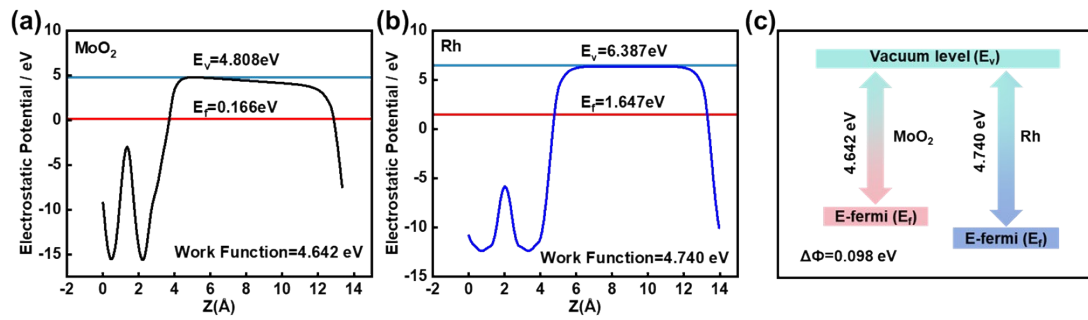


Figure S22 Work function calculation of (a) MoO₂, (b) Rh. (c) Work function diagram between Rh and MoO₂.

Table S1 The fitted parameters of the EIS data of MoO₂-Rh-NF and Rh-NF for HzOR.

Catalysts	Potential / mV	R _s / Ω	R _{ct} / Ω	C / mF
Rh-NF	-0.05	18.01	83.69	0.1045
	0	16.42	147.1	0.09211
	0.05	16.6	106.3	0.0875
	0.1	17.05	33.32	0.0848
	0.15	19.02	19.89	0.0851
MoO ₂ -Rh-NF	-0.05	10.87	32.93	0.1406
	0	10.93	60.88	0.1471
	0.05	10.82	46.22	0.1433
	0.1	10.2	17.51	0.1033
	0.15	10.23	10.28	0.086

Table S2 Comparison of HzOR performance previously reported catalysts.

Catalysts	Electrolyte (1 M KOH +)	Potential / mV (10 mA cm ⁻²)	Tafel slope /mV dec ⁻¹	Ref.
MoO ₂ -Rh-NF	0.3 M N ₂ H ₄	-65	36.0	This work
RhIr MNs	0.5 M N ₂ H ₄	-12	30	1
Rh ₂ S ₃ /NC	0.1 M N ₂ H ₄	95	46	2
Rh/RhO _x -500	0.5 M N ₂ H ₄	-28	33.2	3
Rh/N-CBs	0.05 M N ₂ H ₄	72	74.16	4
RhRu _{0.5} -alloy	1.0 M N ₂ H ₄	-48	/	5
Ru-Cu ₂ O/CF	0.5 M N ₂ H ₄	-41	34	6
PW-Co ₃ N NWA/NF	0.1 M N ₂ H ₄	41	40	7
Ru ₁ -NiCoP	0.3 M N ₂ H ₄	-60	19.3	8
NiIr _{0.03} -BDC	0.3 M N ₂ H ₄	-21	24	9
Rh-SA/Ti ₃ C ₂ O _x	0.1 M N ₂ H ₄	38	40	10

Table S3 Comparison of HER performance previously reported catalysts in 1 M KOH.

Catalysts	Electrolyte	Overpotential / mV (10 mA cm ⁻²)	Ref.
MoO ₂ -Rh-NF	1 M KOH	24.2	This work
RhIr MNs	1 M KOH	20	1
Rh ₂ S ₃ /NC	1 M KOH	38	2
Rh/RhO _x -500	1 M KOH	17	3
Rh/N-CBs	1 M KOH	77	4
Ru-Cu ₂ O/CF	1 M KOH	31	6
PW-Co ₃ N NWA/NF	1 M KOH	41	7
Ru ₁ -NiCoP	1 M KOH	32	8
NiIr _{0.03} -BDC	1 M KOH	27	9
Rh-SA/Ti ₃ C ₂ O _x	0.1 M KOH	29	10

References

- 1 M. Zhang, Z. Wang, Z. Duan, S. Wang, Y. Xu, X. Li, L. Wang and H. Wang, *J Mater Chem A*, 2021, **9**, 18323-18328.
- 2 C. Zhang, H. Liu, Y. Liu, X. Liu, Y. Mi, R. Guo, J. Sun, H. Bao, J. He, Y. Qiu, J. Ren, X. Yang, J. Luo and G. Hu, *Small Methods*, 2020, **4**, 2000208.
- 3 J. Yang, L. Xu, W. Zhu, M. Xie, F. Liao, T. Cheng, Z. Kang and M. Shao, *J Mater Chem A*, 2022, **10**, 1891-1898.
- 4 N. Jia, Y. Liu, L. Wang, P. Chen, X. Chen, Z. An and Y. Chen, *Acs Appl Mater Inter*, 2019, **11**, 35039-35049.
- 5 X. Fu, D. Cheng, C. Wan, S. Kumari, H. Zhang, A. Zhang, H. Huyan, J. Zhou, H. Ren, S. Wang, Z. Zhao, X. Zhao, J. Chen, X. Pan, P. Sautet, Y. Huang and X. Duan, *Adv Mater*, 2023, **35**, 2301533.
- 6 P. Shen, B. Zhou, Z. Chen, W. Xiao, Y. Fu, J. Wan, Z. Wu and L. Wang, *Appl Catal B-Environ*, 2023, **325**, 122305.
- 7 Y. Liu, J. Zhang, Y. Li, Q. Qian, Z. Li, Y. Zhu and G. Zhang, *Nat Commun*, 2020, **11**, 1853.
- 8 Y. Hu, T. Chao, Y. Li, P. Liu, T. Zhao, G. Yu, C. Chen, X. Liang, H. Jin, S.

- Niu, W. Chen, D. Wang and Y. Li, *Angew Chem Int Edit*, 2023, DOI: 10.1002/anie.202308800, e202308800.
- 9 X. Xu, H.-C. Chen, L. Li, M. Humayun, X. Zhang, H. Sun, J. Jia, C. Xu, M. Bououdina, L. Sun, X. Wang and C. Wang, *Adv Funct Mater*, 2024, DOI: <https://doi.org/10.1002/adfm.202408823>, 2408823.
- 10 X. Peng, Y. Mi, X. Liu, J. Sun, Y. Qiu, S. Zhang, X. Ke, X. Wang and J. Luo, *J Mater Chem A*, 2022, **10**, 6134-6145.